J Nanopart Res (2024) 26:154
https://doi.org/10.1007/s11051-024-06060-w

RESEARCH

Enhancing polypropylene composites: synergistic effects of graphene nanoplatelets and glass fibers on mechanical and thermal properties

Giovani B. Berti · Diego Piazza · Bruna F. Bortoli · Rosmary N. Brandalise

Received: 16 January 2024 / Accepted: 23 June 2024 / Published online: 11 July 2024
© The Author(s), under exclusive licence to Springer Nature B.V. 2024

Abstract This study investigates the development of polypropylene (PP) nanocomposites reinforced with graphene nanoplatelets (GNPs) and glass fibers (FGs), focusing on the evaluation of their morphological, thermal, and mechanical properties. Through twin-screw and single-screw extrusion processes followed by injection, we explore the influence of different GNP concentrations (0, 0.125, and 0.5 wt%) and the addition of glass fibers (20, 40, and 60 wt%) on the PP matrix. The results indicate that the careful incorporation of GNP and glass fibers not only significantly enhances the mechanical strength and thermal deflection temperature of the nanocomposites but also affects crystallinity and thermal conductivity in predictable and beneficial ways. Particularly, nanocomposites containing 0.125% GNP and 40% glass fibers exhibited an increase of 254.1% in tensile strength and 243.2% in flexural strength compared to pure PP, highlighting the potential of these materials in high-performance engineering applications. This work not only advances knowledge in the area of polymer nanocomposites but also demonstrates the practical potential of hybrid materials in overcoming the limitations of conventional materials, opening new perspectives for their application in critical sectors such as automotive, aerospace, and construction.

Keywords Graphene nanoplatelets · Polypropylene · Fiberglass · Composites · Extrusion · Injection · Polymer nanocomposites · Increased mechanical performance

G. B. Berti · D. Piazza · R. N. Brandalise (✉)
University of Caxias Do Sul, (Graduate Program in Process Engineering and Technologies), Caxias Do Sul, RS, Brazil
e-mail: rnbranda@ucs.br

G. B. Berti
e-mail: gbberti@ucs.br

D. Piazza
UCSGRAPHENE, Caxias Do Sul, RS, Brazil

B. F. Bortoli
Ford Motor Company, Camaçari, BA, Brazil

Introduction

The constant scientific and technological progress drives the search for innovative developments that include the modification of raw materials, the optimization of production processes, and the diversification of applications. Within this demand, the use of polymer nanocomposites, especially those containing graphene nanoplatelets, silicates, and carbon black, has emerged as a promising strategy [1]. The application of these nanocomposites, in line with the increasing technological development, has opened remarkable opportunities in various sectors such as biomedical engineering, aerospace, petroleum, energy, and automotive industries.[1, 2].

The carbon atom is known for its versatility based on its ability to form bonds in sp, sp [2], and sp [3] hybridized configurations with other atoms, giving it the ability to form a wide range of stable molecules [3].

In particular, carbon nanotubes (CNTs), which consist of hexagonal networks of carbon atoms arranged in tubular structures [4], and graphene nanoplatelets (GNPs), which consist of layers of carbon atoms in sp [2] hybridization organized in a two-dimensional network [5], have attracted considerable attention due to their reinforcing properties, high electrical and thermal conductivity, and corrosion resistance [6].

Based on recent studies, the properties of graphene as a thermal conductor have attracted great interest. This is due to its two-dimensional hexagonal carbon structure and the sp [2] covalent bonds between the carbon atoms. These properties confer thermal conductivity to graphene, although thermal conduction is limited due to the relatively weak van der Waals interactions. Recent studies have shed light on the influence of the average layer thickness of graphene nanoplatelets on their thermal conductivity [7]. It is important to note that clusters of nanoplatelets do not favor this process.

Carbon nanoparticles and their derivatives often exhibit a significant tendency to aggregate, a factor that hinders the full realization of their reinforcing potential in practical applications. To mitigate this cohesion phenomenon and promote effective dispersion, interventions such as chemical functionalization and/or ultrasonic treatment (sonication) are routinely applied to the polymer matrix and/or nanofillers in question [8–12].

The mechanical, electrical, and thermal properties of graphene have attracted considerable attention from the scientific community, highlighting its potential impact on technological innovation [2, 13]. With controlled amounts of graphene nanoplatelets between 0.1 and 1.0 wt%, improvements in tensile strength, an increase in elastic modulus, and improvements in thermal and electrical conductivity can be achieved [14–16].

The thermal conductivity in composites with GNP could be related to the effective dispersion of these nanostructures in the matrix. Appropriate dispersion of nanofillers allows greater heat transfer through the matrix, thus improving the thermal conductivity of the composite. Conventional electron microscopic techniques such as scanning electron microscopy (SEM) can be used to evaluate the morphology of GNP in composites, but are not able to provide accurate information about GNP dispersion. An efficient alternative is to measure the conductivity of the composites and compare them with each other and with the neat (untreated) polymer. [8, 17, 18].

Incorporating GNPs into polymers, as demonstrated by Wijerathne et al. [19], significantly enhances the mechanical and thermal properties of both virgin and recycled polycarbonate nanocomposites. Their research highlighted the critical role of GNPs in improving Young's modulus and yield strength, with notable increases observed at a 10 wt% GNP loading. This foundational work informs our study's exploration into the combined effects of GNPs and glass fibers within a polypropylene matrix, aiming to advance the performance capabilities of polymer nanocomposites further.

Polypropylene (PP) is a thermoplastic used in various fields such as packaging, toys, textiles, and automotive. It is characterized by its versatility, good properties, and ease of processing. However, its performance in highly demanding engineering applications is still limited [20, 21]. Incorporation of nanoparticles into PP may be an alternative to improve its properties and performance. The effectiveness of nanocomposites depends on the type and composition of the nanofiller, the morphology and degree of dispersion of the nanoparticles, and the interactions between the matrix and the nanoparticles [22]. PP—in the last two decades—nanocomposites based on carbon nanoparticles and their derivatives such as CNTs and GNPs have been investigated. These nanocomposites exhibit a number of remarkable mechanical properties as well as electrical and thermal conductivity [8, 23].

Several studies have explored the creation of composites made from PP and GNP, with GNP concentrations ranging from 0.1 to 0.5 weight percent (wt%). These composites were processed using a twin-screw extruder at temperatures between 190 and 210 °C, and they demonstrated a bending elasticity modulus of 1.9 GPa and a bending strength of 36 MPa when the GNP content was under 0.4 wt% [24]. In particular, one study found that composites composed of PP and GNP, manufactured via twin-screw injection molding and incorporating GNP of 25 µm in size and surface areas of 50–80 $m^2 \cdot g$ (with an average thickness of 15 nm) and 120–150 $m^2 \cdot g$ (with an average thickness of 6–8 nm) at concentrations of 1, 2, 3, 4, and 5 wt%, displayed enhanced mechanical properties for both GNP sizes. It was observed that reducing the thickness of the GNP led to a decrease in impact strength but increased both the tensile and bending strength, as well as the elasticity modulus. The highest tensile strength achieved was approximately 33 MPa, and the highest bending strength was about

58.81 MPa, for the composite with 5 wt% GNP of an average thickness between 6 and 8 nm [25].

The automotive industry's developments have sought to improve the efficiency of parts that are now manufactured using high-performance polymers, replacing them with commodities to maintain the unique properties that give products value. Commodities primarily include polyethylene (PE), PP, and polystyrene (PS). This replacement is accomplished through a variety of approaches, including the incorporation of reinforcements into polymer matrices and the use of specific additives to modify processing and properties [26, 27].

In view of the above, this study proposes to investigate the effect of glass fibers (3 mm long) at a concentration of 20, 40, and 60 wt%, together with different concentrations of graphene nanoplatelets (0, 0.125, and 0.5 wt%), in composites previously prepared by twin-screw extrusion and then by single-screw extrusion followed by injection. This approach aims to investigate the morphological, physicochemical, thermal, and mechanical properties of these composites. In summary, the objective of this study is to evaluate the influence of the addition of graphene nanoplatelets and glass fibers and the type of blending process on the properties of polypropylene-based composites.

The incorporation of reinforcing materials, such as glass fibers and GNPs, into polymer matrices constitutes a dynamic and continually advancing area of research, significantly impacting the development of advanced materials engineering. Although the integration of these reinforcements into PP is extensively documented, traditional methodologies have predominantly concentrated on examining their effects in isolation, resulting in a notable gap in understanding their collective impact. This study endeavors to fill this void by investigating the synergistic interactions between graphene nanoplatelets and glass fibers within a PP matrix, with the objective of uncovering complex interplays that yield substantial enhancements in the mechanical and thermal properties of the resulting composites.

This research distinguishes itself through a methodical examination of the interactions between GNP and glass fibers, as well as their combined effects on the properties of the PP composite. Utilizing advanced characterization techniques, this study has elucidated not only the improved distribution and dispersion of these reinforcements within the PP matrix but also the fundamental mechanisms at the reinforcement-matrix interface contributing to enhanced material performance. These insights provide significant contributions to the field of polymer nanocomposites, establishing innovative paradigms for the design of composite materials and facilitating the emergence of new applications across diverse engineering fields.

Accordingly, this work contributes to a deeper understanding of polymer nanocomposites and illustrates the practical advantages of strategically integrating multiple reinforcements to surmount the constraints of traditional materials. The implications of these findings are extensive, encouraging the development of novel polymer composites with tailored properties to fulfill specific performance and sustainability criteria in critical applications, spanning the automotive to aerospace industries and beyond.

Experimental

Materials

The polypropylene, type CP 442XP copolymer, was supplied by Braskem®, density of 0.895 g cm^{-3}, flowability index of 6.0 g 10 min^{-1}. The type S glass fibers were supplied by Owens Corning®, have a nominal filament diameter of 14 µm and a nominal length of 3 mm, and are surface treated with organosilane. The graphene nanoplatelets are from UCS-GRAPHENE®, code UGZ-1004, in powder form, with a carbon composition of up to 96.9 wt%, a specific surface area (calculated according to the multimolecular adsorption theory of Brunauer, Emmett, and Teller (BET)) of 26.09 m^2 g^{-1}, with the highest frequency in the film distribution curve between 12 and 15. The adhesion promoter used was Polybond 3200, purchased from Addivant®.

Manufacturing

The composites were prepared in the compositions given in Table 1. The raw material was first dried in an oven model TE-394/2 from Tecnal (Brazil) and then extruded in an interpenetrating co-rotating twin screw model MH-COR-20–32-LAB from MH Equipments (Brazil) with L/D 45.25 and a diameter of 20 mm, a speed of 200 rpm, and a temperature profile of 160 to 190 °C. The material was then pelletized

Table 1 Composition and coding of nanocomposites

Sample	PP (% wt/wt)	CA (% wt/wt)	GNP (% wt/wt)	FG (% wt/wt)
PPv	100.0	0.0	0.0	0.0
PP/GNP0/FG0	98.0	2.0	0.0	0.0
PP/GNP0/FG20	78.0	2.0	0.0	20.0
PP/GNP0/FG40	58.0	2.0	0.0	40.0
PP/GNP0/FG60	38.0	2.0	0.0	60.0
PP/GNP0125/FG0	97.875	2.0	0.125	0.0
PP/GNP0125/FG20	77.875	2.0	0.125	20.0
PP/GNP0125/FG40	57.875	2.0	0.125	40.0
PP/GNP0125/FG60	37.875	2.0	0.125	60.0
PP/GNP050/FG0	97.5	2.0	0.50	0.0
PP/GNP050/FG20	77.5	2.0	0.50	20.0
PP/GNP050/FG40	57.5	2.0	0.50	40.0
PP/GNP050/FG60	37.5	2.0	0.50	60.0

PPv virgin PP processed in twin-screw, *CA* compatibilizing agent, *GNP* graphene nanoplatelets, *FG* fiberglass

and dried at 80 °C for 4 h. The PP, coupling agent, and NPG were added to the twin screw in three different stages. The glass fibers were incorporated in mass fractions of 20, 40, and 60% in the composite coming from the twin screw, in a Seibt (Brazil) single-screw extruder, model ES35 F-R, with L/D 32 and diameter 35 mm, at process parameters 160 °C in feed to 210 °C and at a speed of 50 rpm. The material was then pelletized and injected into a Himaco (Brazil) model LH 150–80 injection molding machine with an L/D of 18.3 and a diameter of 40 mm, with a temperature profile that varied from 170 to 190 °C.

Figure 1 shows the processing flow of the composites in this study.

Characterization methods

Prior to characterization testing, samples were conditioned at 23 °C and 50% relative humidity for 48 h.

Thermal properties

ASTM D3418-21 standard was used to perform differential scanning calorimetry (DSC) analyzes on a Shimadzu (Japan) model DSC50 instrument at an N_2 flow of 50 mL min^{-1} and a rate of 10° C min^{-1} from 23 to 250 °C. The crystallinity index (X_c) of the samples was determined using Eq. 1.

$$Xc = \frac{1}{n}\left(\frac{\Delta Hf}{\Delta Hf\ 100\ \%}\right) \times\ 100\ \% \quad (1)$$

Where $\Delta Hf_{100\%}$ is the enthalpy of fusion of the hypothetical 100% crystalline PP, corresponding to 209 J g^{-1} [28], and ΔHf is the enthalpy of fusion of the polymer, normalized ($1/n$) with respect to its incorporated content in the composite in J g^{-1}.

Heat deflection temperature (HDT) was evaluated according to ASTM D468-18 up to 0.25-mm deflection and 1.8-MPa load. The used equipment of the VICAT model was from the brand Instron (Norway). Three specimens of each sample were evaluated.

The thermal conductivity of the composites was measured according to ASTM C518-17 standard in an environment with a controlled temperature of 23 ± 2 °C and humidity of 50%. The specimens were placed between two plates: The upper plate (T_1), which has electrical resistance and temperature control, was heated to 60 °C, while the lower plate (T_2) remained at 23 ± 2 °C. Thermocouples are attached to both plates and connected to a temperature gage. During the test, the temperatures of both plates (T_1 and T_2) are recorded every 10 min until the temperature variations of the two plates and their heat transfer have stabilized for at least five measurements. To avoid heat loss, the system is insulated by glass plates and asbestos blocks. The calibration of the device was performed with glass wool, whose thermal conductivity value (k) is 0.038 W m^{-1} K^{-1} [29] at a thickness of 0.0215 m, to determine the heat flux of the system (q^0).

The heat flux of the system (q^0) was determined by the Eq. 1 (2).

$$q^0 = -k.A.\frac{dT}{dx} \quad (2)$$

where q^0 is the heat flow of the system in W m^{-2}; k is the thermal conductivity coefficient of the sample in W m^{-1}·K^{-1}; ɖT is the temperature variation (T_1–T_2) in K; ɖx is the thickness of the sample in m.

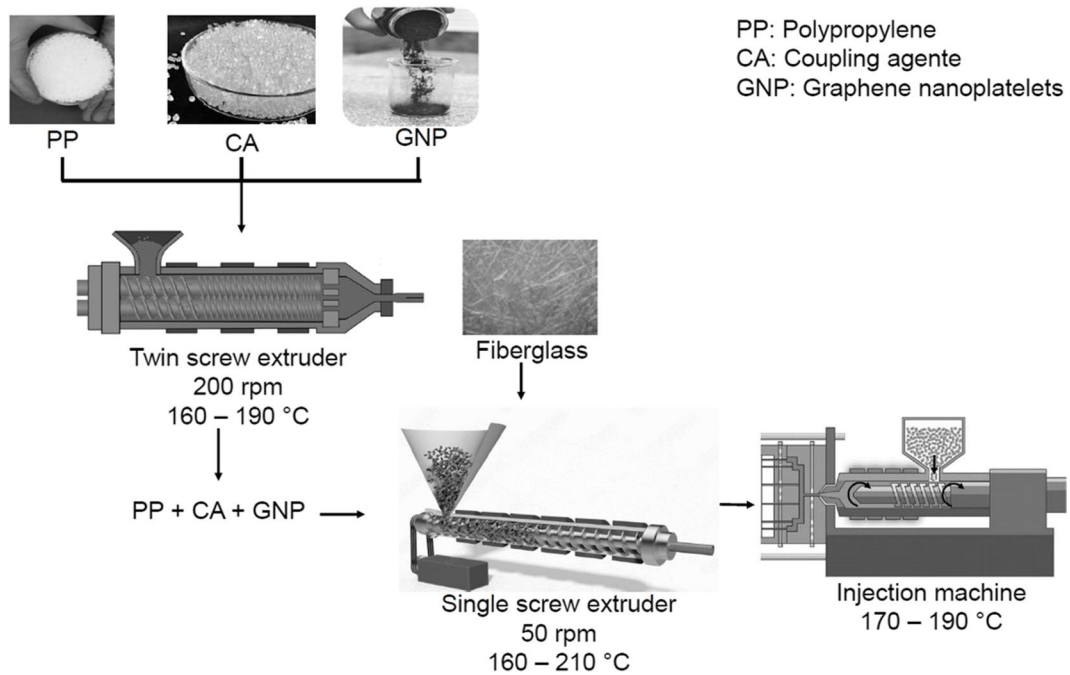

Fig. 1 Processing flow of the composites in this study

When the heat flux through the glass layer is defined, a new sample is inserted into the system. Heat transfer is expected to stabilize and the thermal conductivity (k) of the remaining samples is calculated using Eq. 3.

$$k = ((q.L)/\Delta T) \quad (3)$$

Given k as the thermal conductivity coefficient of the sample ($W.m^{-1}.K^{-1}$); q as the heat flux of the system ($W.m^{-2}$); L as the thickness of the sample (m); and ΔT as the temperature variation (T_1–T_2) (Kelvin).

Morphological properties

The morphology of the samples was analyzed by field emission scanning electron microscopy (SEM/FEG), breaking them with liquid nitrogen and coating them with gold (sputtering). The images were acquired at magnifications of 250× and 5000×. The instrument used is of the brand Tescan (Czech Republic), model MIRA3. The cross-section of the specimens from the mechanical bending tests after cryogenic fracture was used for this evaluation.

Mechanical properties in thermoplastic standards adapted to composites

The flexural strength tests were performed according to ASTM D790-17 standard with a load cell of 2000 kgf and a speed of 50 mm min^{-1} on an Emic device, model DL200 (Brazil). The tensile strength tests were carried out according to the ASTM D638-14 standard at a speed of 50 mm min^{-1} and a load cell of 2000 kgf in the previously mentioned device. In each test, five samples of each specimen were evaluated.

Fiber content and fiber size distribution after single-screw and injection processing

The ash content was determined by calcining the samples according to ASTM D5630-22 standard in triplicate in a Fornitec (Brazil) brand furnace at a temperature of 800 °C for a period of 5 min, followed by cooling in a desiccator and weighing.

The size distribution of the glass fibers from the calcination of the samples was evaluated using an optical microscope from Opticam (Brazil) in

conjunction with ImageJ software. The samples were characterized after processing by single-screw extrusion and after injection of the samples.

Results and discussion

Characterization of thermal properties

Table 2 shows the parameters obtained from the DSC and HDT tests. From the DSC, it was found that an increase in X_c from 31.3 to 37.3% was observed for the sample processed only with the twin screw (PP_v) and the PP/GNP0/FG0 that came from the twin screw, followed by the single screw. This increase can be attributed to the degradation of PP by β-cleavage, which leads to greater mobility of the polymer chains, promotes a more ordered arrangement, and consequently favors the formation of crystalline structures upon cooling [30]. Compared to other composites, an inversely proportional relationship was observed between X_c of the samples and the incorporated FG content. This phenomenon is related to the spatial obstruction by the fibers, which limits the formation of PP crystallites for the composite. This observation is consistent with the results reported in the literature with PP and 50% FG [30, 31]. This trend remained consistent regardless of variations in GNP content and a possible effect of GNP as a nucleating agent, with the incorporated FG content being the most influential factor in this context.

When considering the presence of GNP in the samples PP/GNP0/FG0, PP/GNP0125/FG0, and PP/GNP050/FG0, it was found that the T_m value was 167 °C. Therefore, the presence of graphene in the composites processed by single-screw extrusion did not affect this parameter. The same result was observed for PP_v processed by twin-screw extrusion without using a compatibilizer. No significant differences in T_m values were observed between the composites when varying the mass fractions used (20, 40, and 60 wt%). This behavior confirms what has already been reported in the literature about the addition of 50% long glass fibers with a diameter of 14 µm in a polypropylene copolymer matrix [31].

Based on the data for HDT presented in Table 2, an increase in HDT was observed for composites with 20% FG, which was associated with an increase in X_c. Above this fiber content, the increase in HDT is more influenced by the presence of the fiber; as the X_c values decrease, as previously highlighted, the fibers affect the formation of crystals. The best HDT result was obtained with the composite PP/GNP0125/FG40. In the literature, polypropylene composites reinforced with different FG contents between 0 and 26% show an increase in HDT according to the addition of FG to the composite, as demonstrated in the present study [32].

The reason for increasing HDT and decreasing crystallinity in polymer composites with FG is due to the interaction between the fibers and the polymer matrix. FG acts as nucleation sites for crystal formation, which can increase the crystallinity of the composite. However, the presence of glass fibers can also restrict the mobility of the polymer chains, leading to a decrease in crystallinity in the vicinity of the fibers. The increase in HDT is due to the reinforcement of the polymer matrix by the FG, which improves the composite's resistance to deformation under heat and load. The decrease in crystallinity can be attributed to the fact that the FG hinder the crystallization of the polymer matrix, leading to a less ordered structure [33, 34].

Table 2 Parameters obtained from the DSC (1st complete run) and HDT techniques

Sample	T_m (°C)	X_c (%)	HDT (°C)
PPv	167.8	31.0	49.3 ± 0.9
PP/GNP0/FG0	167.3	37.3	51.4 ± 1.1
PP/GNP0/FG20	167.3	31.3	138.7 ± 2.4
PP/GNP0/FG40	167.1	23.0	142.1 ± 3.3
PP/GNP0/FG60	168.1	13.5	147.9 ± 2.4
PP/GNP0125/FG0	167.7	34.3	49.9 ± 1.7
PP/GNP0125/FG20	167.2	28.0	140.1 ± 4.0
PP/GNP0125/FG40	167.2	21.0	147.8 ± 0.7
PP/GNP0125/FG60	166.4	16.6	149.2 ± 1.7
PP/GNP050/FG0	167.1	34.6	47.4 ± 0.9
PP/GNP050/FG20	167.4	26.9	138.1 ± 5.3
PP/GNP050/FG40	166.6	22.8	146.2 ± 2.7
PP/GNP050/FG60	167.1	16.3	147.4 ± 2.1

GNP dispersion and thermal conductivity

Table 3 shows the results of thermal conductivity of the studied samples. In the analysis of thermal conductivity, the thermal conductivity was considered

Table 3 Thermal conductivity results of the samples

Sample	Average sample thickness (m)	Thermal conductivity ($W\ m^{-1}\ K^{-1}$)
Glass wool	0.0200	0.03800*
PPv	0.0032	0.01093
PP/GNP0/FG0	0.0034	0.01347
PP/GNP0/FG20	0.0029	0.01035
PP/GNP0/FG40	0.0033	0.01019
PP/GNP0/FG60	0.0028	0.01007
PP/GNP0125/FG0	0.0032	0.01652
PP/GNP0125/FG20	0.0035	0.01631
PP/GNP0125/FG40	0.0031	0.01656
PP/GNP0125/FG60	0.0029	0.01433
PP/GNP050/FG0	0.0032	0.01483
PP/GNP050/FG20	0.0032	0.01427
PP/GNP050/FG40	0.0033	0.01393
PP/GNP050/FG60	0.0034	0.01471

*k of glass wool = 0.038 [[29]]

relative rather than absolute to allow a comparative evaluation between the samples in this study. This care is due to two aspects: First, we tried to use both the standard sample as a thermal insulator and the study samples, and second, due to the different thicknesses between the standard glass wool sample and the thickness of the study samples.

An increase in thermal conductivity was observed for the samples with graphene nanoplatelets compared to the samples without graphene, with higher values for the samples with 0.125% GNP weight. The different contents of FG did not affect the thermal conductivity, contrary to what has been demonstrated in the literature, where glass fibers caused a decrease in the thermal conductivity of samples with graphene nanoplatelets for epoxy composites reinforced with graphene nanoplatelets, graphene oxide, and reduced graphene oxide [35].

In the studies of Su et al. [17] and Xiao et al. [18], GNPs, when properly dispersed in the polymer matrix, are able to form conductive contact networks for heat and thus exert a direct influence on the thermal conductivity of the nanocomposite. The agglomeration of GNP has an opposite effect on the thermal conductivity of the composite. The greater the degree of agglomeration of the GNPs, the lower the thermal conductivity. This is due to the decrease of favorable contact areas and the increase of inefficiency in thermal conduction. These results highlight the promising potential of GNPs to improve the thermomechanical properties of polymer composites.

According to the observations and taking into account the recommendations in the literature [17, 18], a better dispersion of the nanoplatelets in the polypropylene matrix was achieved in the composites with 0.125% GNP.

Figure 2a shows the preferred paths for heat conduction through the GNP dispersion and in Fig. 2b the clusters of graphene nanoplatelets.

Characterization of morphological properties

Figure 3a–l display the SEM micrographs at 250× magnification.

Figure 3a–l show that the fibers are arranged both transversely and longitudinally to the fracture surface. Sample PP/GNP0/FG0 exhibited a rough surface, but with smaller protrusions than samples (e) PP/GNP0125/FG0 and (i) PP/GNP050/FG0, without the presence of FG. Corresponding to the increase of fibers in the composites, the presence of fibers in the matrix also increased significantly. With the incorporation of graphene nanoplatelets, a better dispersion of fibers in the matrix was observed without the

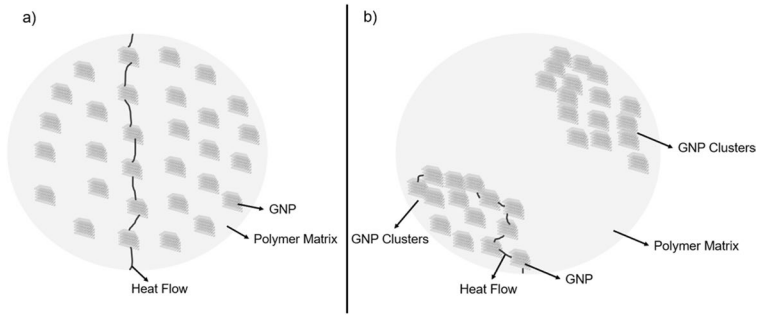

Fig. 2 Thermal conductivity of the studied samples; **a** preferred pathways for thermal conduction through dispersed GNP; **b** agglomerated, difficulties in thermal conduction in the polymer matrix. [17] Adapted from Su et al.

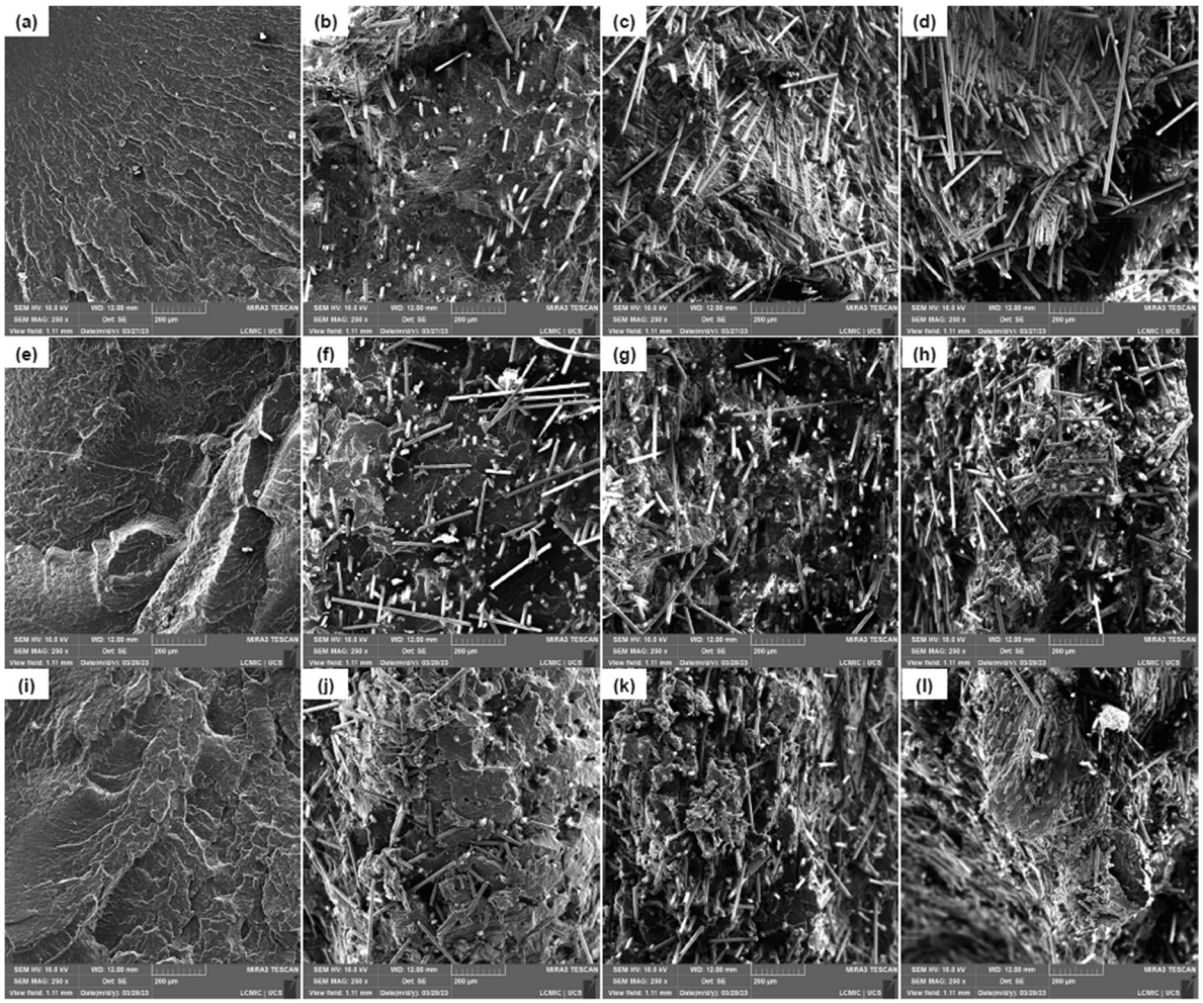

Fig. 3 Micrographs obtained from SEM with magnification of 250×. **a** PP/GNP0/FG0; **b** PP/GNP0/FG20; **c** PP/GNP0/FG40; **d** PP/GNP0/FG60; **e** PP/GNP0125/FG0; **f** PP/GNP0125/FG20; **g** PP/GNP0125/FG40; **h** PP/GNP0125/FG60; **i** PP/GNP050/FG0; **j** PP/GNP050/FG20; **k** PP/GNP050/FG40; **l** PP/GNP050/FG60

accumulations visible in samples (c) PP/GNP0/FG40 and (d) PP/GNP0/FG60. Based on the dispersion aspect and fiber agglomerates, the best morphology was attributed to the samples with 0.125 wt% graphene nanoplatelets (Fig. 3g).

Figure 4a–i show the microscopic images obtained from SEM at 5000×magnification. Analysis of Fig. 4a–i revealed good interfacial adhesion of the PP matrix in the FG coating. This good matrix/fiber interface was attributed to the compatibilizer present in all samples and to the fact that the glass fiber was treated with organosilane, a result not presented in this study, without demonstrating the effect of GNP on enhancing the reinforcement/matrix interaction [36].

Graphene and its derivatives have a variety of properties that make it an effective processing aid. It has a large surface area, chemical stability, thermal and electrical conductivity, high hydrophobicity, flexibility, and more. These properties make it possible to combine the nanoscale features of graphene with concrete applications at the macroscopic scale [37]. Regarding the interaction between matrix and fibers, in a study with an admixture of 0 to 7 wt% GNP and 0 to 30 wt% FG in a PP matrix, GNP contributed to the reinforcement and interaction between fibers and matrix [38], which could not be demonstrated in the present study.

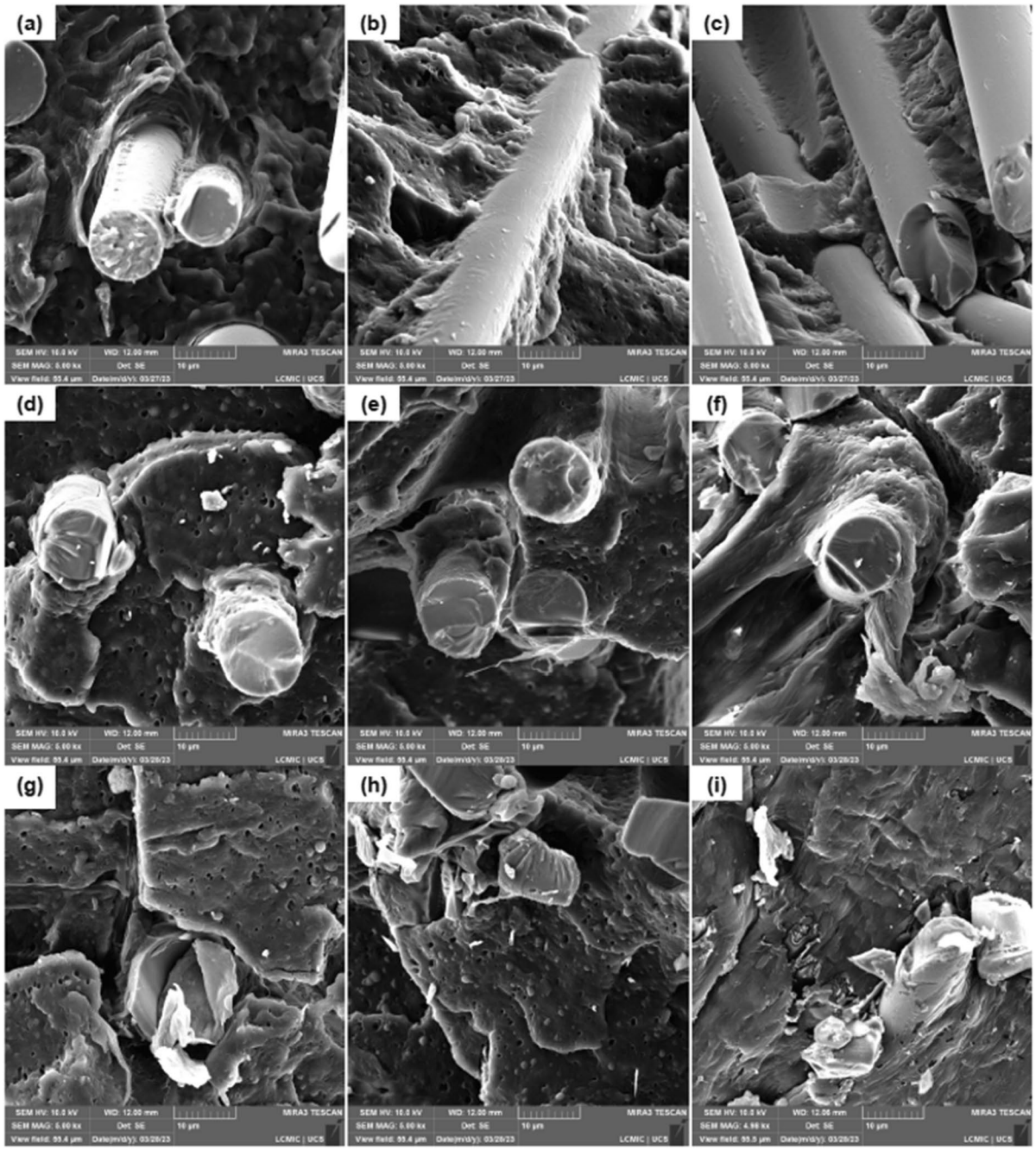

Fig. 4 Micrographs obtained from SEM at 5000 × magnification; **a** PP/GNP0/FG20; **b** PP/GNP0/FG40; **c** PP/GNP0/FG60; **d** PP/GNP0125/FG20; **e** PP/GNP0125/FG40; **f** PP/GNP0125/FG60; **g** PP/GNP050/FG20; **h** PP/GNP050/FG40; **i** PP/GNP050/FG60

Characterization of mechanical properties

Figure 5 shows the results of tensile strength, modulus of elasticity in tension, and flexural strength of the composites. Regarding the tensile strength, no significant differences were found between the specimens with and without GNP, which is consistent with the literature, since only small amounts of GNP were

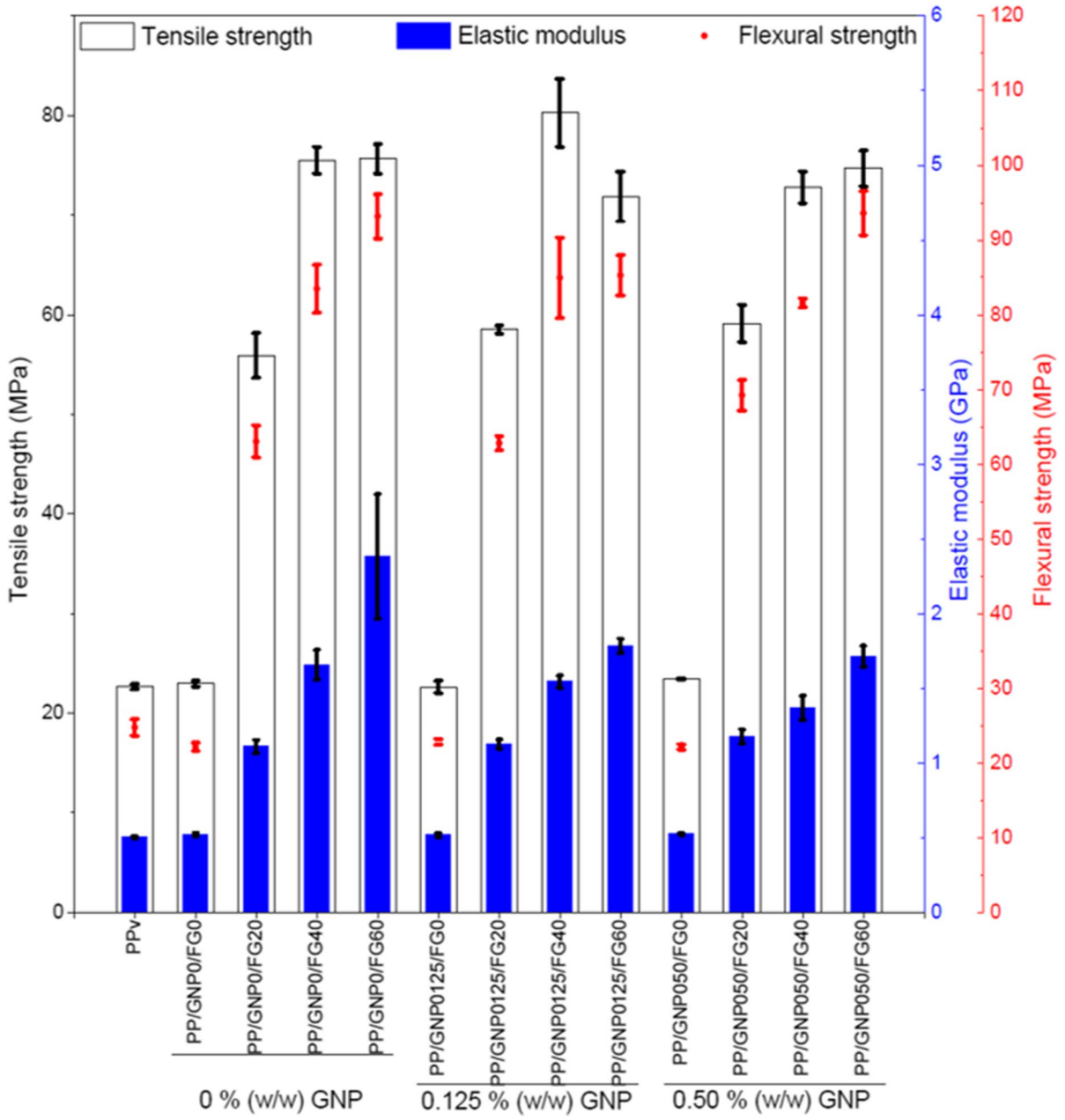

Fig. 5 Tensile strength, tensile modulus of elasticity, and flexural strength of composites

used and the incorporation process was via a twin-screw extruder.[39].

Tensile strength and elastic modulus were found to increase with the addition of FG, but this increase reached a limit at 40% FG. Additions greater than 40% FG did not result in an increase in tensile strength, which is consistent with a previous study [40] that showed a constant increase in tensile strength of polymer composites up to an incorporated fiber concentration of 20% wt.

Fibers can improve the mechanical resistance of composites, but it is the polymer matrix role to protect them from damage and distribute them well [41]. Excess reinforcing material can result in a less effective

composite, as observed in specimens PP/GNP0/FG60, PP/GNP0125/FG60, and PP/GNP050/FG60, where the polymer matrix does not effectively cover all fibers.

As with tensile strength, the modulus of elasticity determined in the tensile test did not vary with GNP content, but with FG content. The specimen PP/GNP0/FG60 achieved the best performance with a result of 2.4 ± 0.4 GPa.

The incorporation of FG into polymer composites resulted in an increase in tensile strength and elastic modulus due to the better mechanical properties of the fibers, which contributed to a higher strength-to-weight and stiffness-to-weight ratio [42].

When analyzing the results of flexural strength (Fig. 5), it was found that the samples without FG did not differ from each other, as well as the samples PP_v and PP/GNP0/FG0, PP/GNP0125/FG0, and PP/GNP050/FG0, where the performance did not differ significantly. This can be explained by the amount of GNP added to the composite, which can affect the flexural strength, and by the thickness of the GNP, which can affect its effectiveness as a reinforcing agent. GNP with thickness greater than 8 nm have lower flexural strength due to the decrease in stress transfer efficiency due to the lower interaction between fiber and matrix [42, 43]. In the present study, the nanoplatelets are 0.34 nm thick on average, which is smaller than previous studies [42].

The results of flexural strength increased proportionally to the percentage of FG in the composites, with the best results obtained for composites with a mass fraction of 60%, due to the greater stiffness of the matrix/fiber system [44, 45]. The flexural strength of polymer composites increases with the addition of glass fibers due to the mechanical properties of the fibers, which act as a stress-resisting component and improve the overall mechanical strength [46, 47].

As can be seen in Fig. 5, the incorporation of 40 wt% FG and 0.125 wt% GNP resulted in the best tensile strength, with the sample PP/GNP0125/FG40 standing out with 80.3 ± 3.4 MPa. This represents an increase of 254.1% over the PP_v sample and 10.3% over the PP/GNP0/FG40 sample. As for flexural strength, the PP/GNP050/FG60 sample exhibited the highest strength of 93.6 ± 2.9 MPa, corresponding to an increase of 278.1% compared to the PP_v sample.

Figure 6 illustrates the effect of fibers in the tensile strength and flexural strength tests. These properties provide different responses for fiber-reinforced composites, with the resistance of the fibers being more effective in situations of bending as an external action, while in the tensile strength test the interaction between matrix and reinforcement can be evaluated more effectively, as already reported in the literature [48, 49].

Size distribution of fibers after processing in a single-screw extruder (fillets) and injection in the evaluation of test samples

Figure 7 shows the distributions of fiber sizes after single-screw processing and their average size for the samples (a) PP/GNP0/FG20; (b) PP/GNP0/FG40; (c) PP/GNP0/FG60; (d) PP/GNP0125/FG60; (e) PP/GNP050/FG20; (f) PP/GNP050/FG40; and (g) PP/GNP050/FG60.

The properties of composites are also determined by the extent of fiber breakage. Maximizing the fiber length has a significant effect on the final

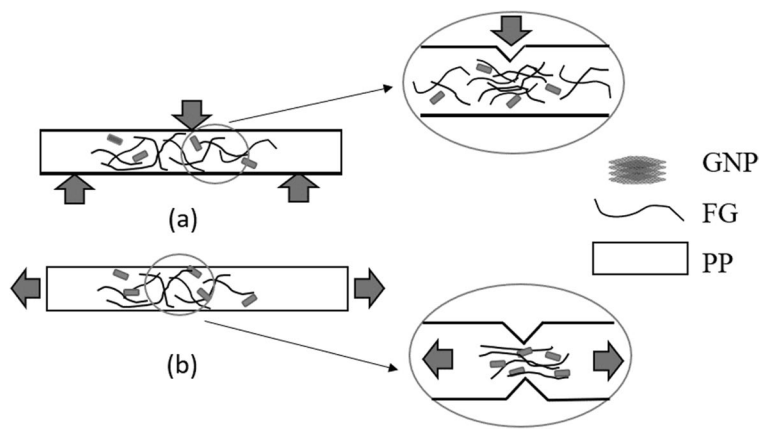

Fig. 6 Illustration of the effect of fibers in a test of **a** flexural strength and **b** matrix/fiber interaction in a tensile strength test

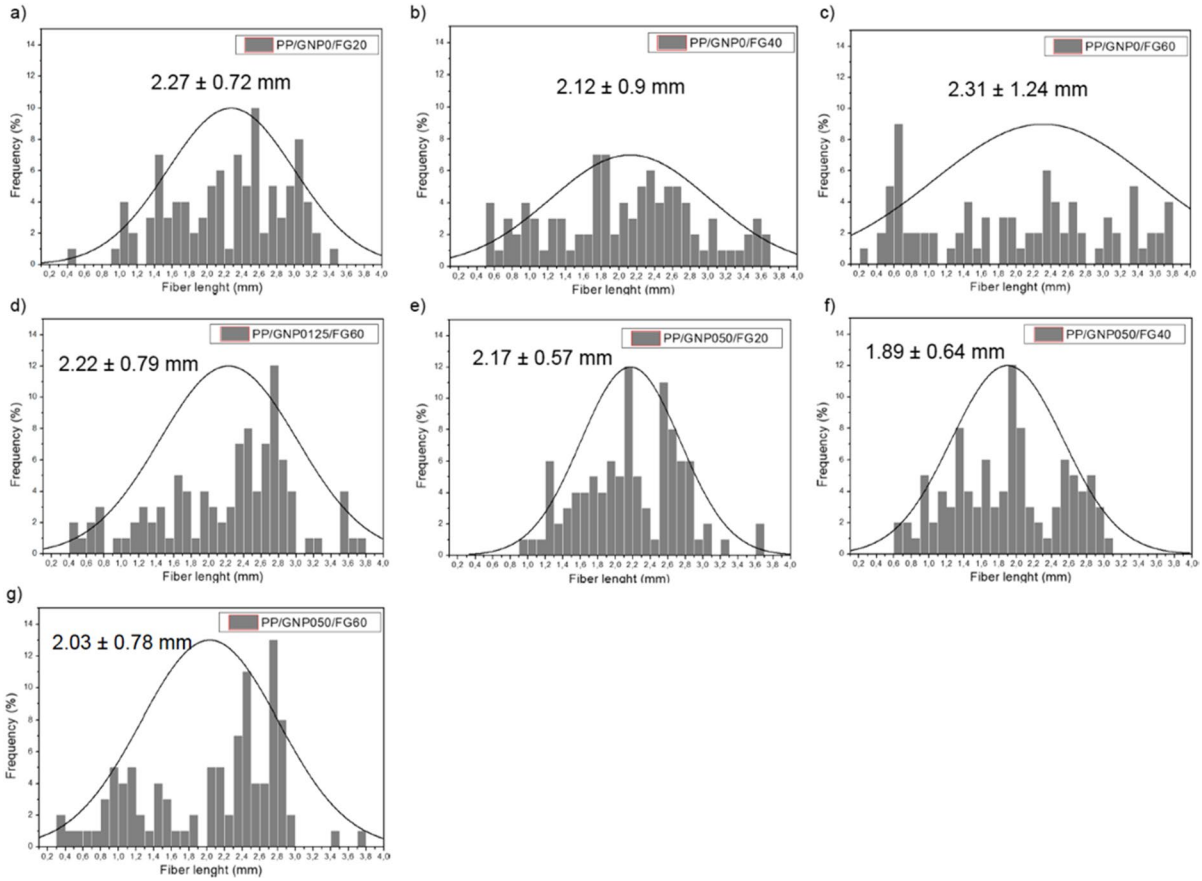

Fig. 7 Fiber size distributions after single-screw processing and their average size for the samples; **a** PP/GNP0/FG20; **b** PP/GNP0/FG40; **c** PP/GNP0/FG60; **d** PP/GNP0125/FG60; **e** PP/GNP050/FG20; **f** PP/GNP050/FG40; **g** PP/GNP050/FG60

physical properties of the composite. Therefore, in the analysis of Fig. 7, it was found that the FGs had an average reduction in size of 28.5% after the single-screw extrusion process. During extrusion, the shear between the screw and the walls of the extruder is directly related to the breakage of the glass fibers and is the factor that most affects the reduction in fiber length during this process [48]. The loss of fiber integrity can also occur at the exit through the matrix.

Figure 8 shows histograms of the distribution of fiber sizes and their average size after processing in the single-screw extruder and after injection, with samples of (a) PP/GNP0/FG20; (b) PP/GNP0/FG40; (c) PP/GNP0/FG60; (d) PP/GNP0125/FG20; (e) PP/GNP0125/FG40; (f) PP/GNP0125/FG60; (g) PP/GNP050/FG20; (h) PP/GNP050/FG40; and (i) PP/GNP050/FG60.

Based on Fig. 8, it was found that the FGs had an average reduction of 74.3% after single-screw extrusion and injection molding. In addition, it is important to highlight that all samples, regardless of the FG content used, exhibited fiber breaks after the extrusion and injection molding phases. Extrusion and injection molding processes can lead to a reduction in the dimensions of glass fibers when they are incorporated into a composite material. This is due to the shear forces that occur in these different processes [50, 51]. In a study of hybrid sisal-glass fiber biocomposites reinforced with 30 wt% PP fibers, a reduction of 87.8 and 95.4% was found after the twin-screw extrusion process and the injection molding process, respectively [51]. The twin-screw extrusion process has a higher shear effect than the single-screw extrusion process, which may have influenced the higher

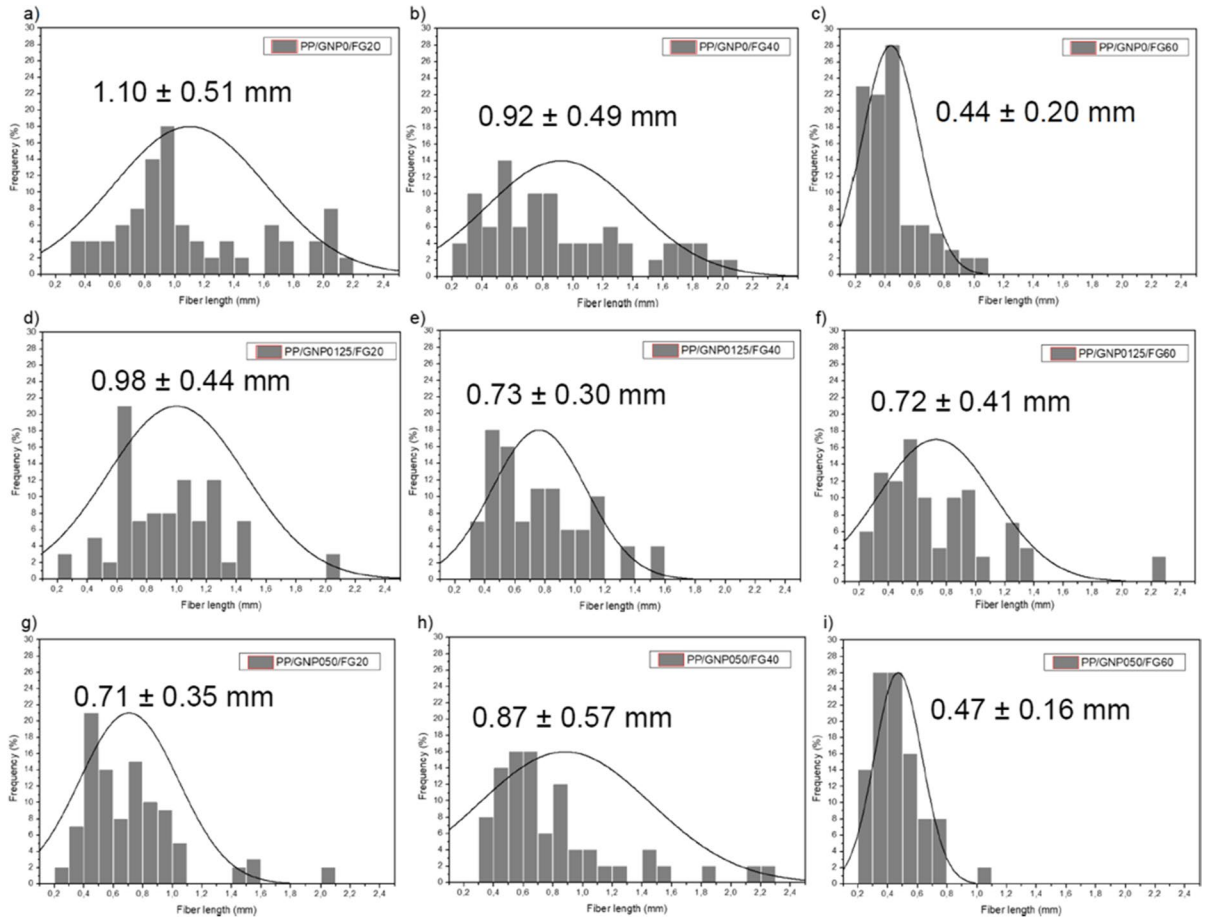

Fig. 8 Histogram of the distribution of fiber sizes and their average size after processing in the single-screw extruder and after injection to evaluate the samples: **a** PP/GNP0/FG20; **b** PP/GNP0/FG40; **c** PP/GNP0/FG60; **d** PP/GNP0125/FG20; **e** PP/GNP0125/FG40; **f** PP/GNP0125/FG60; **g** PP/GNP050/FG20; **h** PP/GNP050/FG40; **i** PP/GNP050/FG60

dimensional loss values in the literature compared to the values in the present study.

In illustrating a single-screw extruder, Fig. 9a, and an injection molding machine Fig. 9b, we found that the glass fibers in the passages of the composite at the beginning of the compression zone are susceptible to integrity loss because the polymer is not fully melted and the interaction between the matrix and fibers is less efficient. During the compression zone during extrusion and injection, the fiber is more exposed to shear from the processes, which increases fracture. Another possible point that can lead to the breakage of FG is the activation of the check valve. Finally, another possible point in the process that affects fracture is the injection nozzle, as it narrows the passage of the molten material. All these signs contribute to the loss of integrity of the glass fibers.

Conclusion

In this investigation, we explored the synergistic reinforcement of polypropylene (PP) with graphene nanoplatelets (GNPs) and glass fibers (FG) through extrusion and injection molding, aiming to enhance the material's performance for high-end applications. Our findings revealed a nuanced interplay between the fillers and the PP matrix, particularly in their thermal and mechanical behaviors. Although GNP's inclusion did not markedly alter the melting temperature (T_m) of

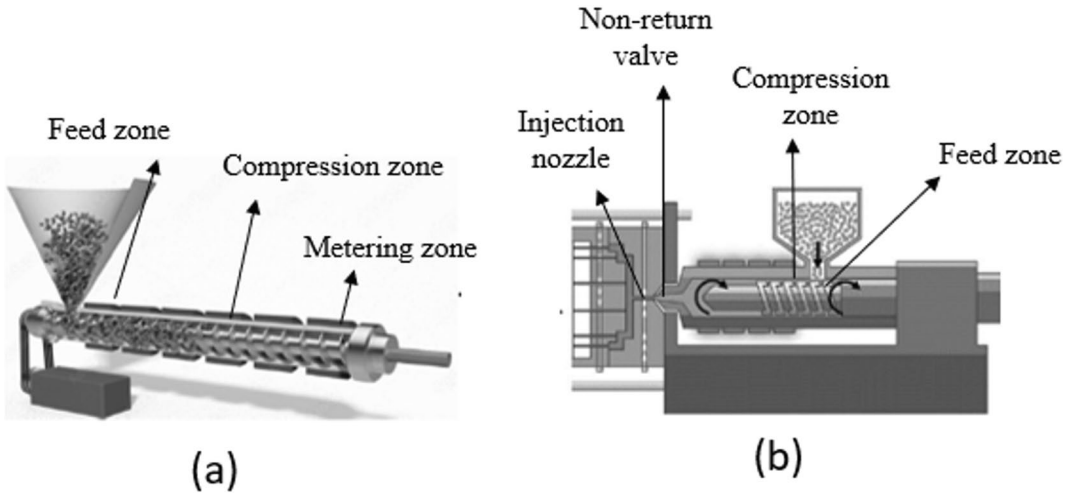

Fig. 9 **a** Schematic representation of parts of a single-screw extruder and **b** schematic representation of parts of an injection molding machine

the composites, introducing FG notably boosted the heat deflection temperature (HDT), with a remarkable increase of 202.6% observed in the PP/GNP0.125/FG60 sample compared to virgin PP. This suggests a superior thermal stability imparted by FG, beneficial for applications requiring high temperature resistance.

Further, the optimal graphene concentration was identified at 0.125 wt%, which demonstrated an excellent dispersion within the PP matrix, thereby enhancing thermal conductivity. This concentration emerged as the most effective, striking a balance between performance improvement and material efficiency. Mechanical testing underscored the enhanced strength and stiffness achievable with 40% FG and 0.125 wt% GNP, showing increases of 253.7% in tensile strength and 210% in elastic modulus relative to virgin PP. These enhancements validate the hypothesis of effective dispersion and synergistic reinforcement.

Moreover, composites with 60 wt% FG exhibited notable improvements in flexural strength, further corroborating the beneficial role of FG in reinforcing the PP matrix. Morphological analyses through SEM confirmed the effective interfacial bonding between the matrix and the fillers, which is pivotal for the observed enhancements in mechanical properties.

Conclusively, our study underscores the exceptional potential of combining graphene nanoplatelets and glass fibers to fortify polypropylene, achieving composite materials with markedly superior properties. This combination not only elevates the material's performance thresholds but also broadens the scope for its application across various industrial sectors. By fine-tuning the concentrations of GNP and FG, we unveil a path toward engineering polypropylene composites that could revolutionize product designs in automotive, aerospace, and beyond, leveraging their enhanced strength, thermal stability, and functional adaptability.

Acknowledgements The authors thank the National Council for Scientific and Technological Development (CNPq), Ford Motor Company Brazil and University of Caxias do Sul (UCS).

Author contribution All authors contributed to the conception, methodology, and design of the study. Data curation, formal analysis, visualization, and the writing of the original draft were performed by Giovani B. Berti. The investigation, review, and editing of the manuscript were conducted by Giovani B. Berti and Rosmary N. Brandalise. Funding acquisition was managed by Diego Piazza. The project was administered by Rosmary N. Brandalise. All authors have read and approved the final manuscript.

Funding This work was financially supported by the National Council for Scientific and Technological Development (CNPq), Ford Motor Company Brazil and University of Caxias do Sul (UCS).

Data availability The data that support the findings of this study are available on request from the corresponding author.

Declarations

Compliance with ethical standards.

Ethical approval It is not applicable for this work.

Conflict of interest The authors declare no competing interests.

References

1. Silva GC, Ladeira GF, Nascimento Júnior H, Carneiro JR (2019) Estudo da substituição do nylon por compósito de polipropileno com fibra de vidro. Mater (Rio Janeiro) 24(3). https://doi.org/10.1590/s1517-707620190003.0737
2. Niyobuhungiro D, Hong L (2021) Graphene polymer composites: review on fabrication method, properties and future perspectives. Adv Sci Technol Res J 15(1):37–49. https://doi.org/10.12913/22998624/129680
3. Li Y, Zhu J, Wei S et al (2011) Poly(propylene) nanocomposites containing various carbon nanostructures. Macromol Chem Phys 212(22):2429–2438. https://doi.org/10.1002/macp.201100364
4. Breuer O, Sundararaj U (2024) Big returns from small fibers: a review of polymer/carbon nanotube composites. Polym Compos 25(6):630–645. https://doi.org/10.1002/pc.20058
5. Li Y, Zhu J, Wei S, Ryu J, Sun L, Guo Z (2011) Poly(propylene)/graphene nanoplatelet nanocomposites: melt rheological behavior and thermal, electrical, and electronic properties. Macromol Chem Phys 212(18):1951–1959. https://doi.org/10.1002/macp.201100263
6. Chen X, Wei S, Yadav A et al (2011) Poly(propylene)/Carbon nanofiber nanocomposites: ex situ solvent-assisted preparation and analysis of electrical and electronic properties. Macromol Mater Eng 296(5):434–443. https://doi.org/10.1002/mame.201000341
7. Wang J, Li C, Li J, Weng GJ, Su Y (2021) A multiscale study of the filler-size and temperature dependence of the thermal conductivity of graphene-polymer nanocomposites. Carbon. https://doi.org/10.1016/j.carbon.2020.12.086
8. Kuilla T, Bhadra S, Yao D, Kim NH, Bose S, Lee JH (2010) Recent advances in graphene based polymer composites. Prog Polym Sci 35(11):1350–1375. https://doi.org/10.1016/j.progpolymsci.2010.07.005
9. Zhong J, Isayev AI, Zhang X (2016) Ultrasonic twin screw compounding of polypropylene with carbon nanotubes, graphene nanoplates and carbon black. Eur Polym J 80:16–39. https://doi.org/10.1016/j.eurpolymj.2016.04.028
10. Arrigo R, Bellavia S, Gambarotti C, Dintcheva NT, Carroccio S (2017) Carbon nanotubes-based nanohybrids for multifunctional nanocomposites. J King Saud Univ Sci 29(4):502–509. https://doi.org/10.1016/j.jksus.2017.09.007
11. Li CQ, Zha JW, Long HQ, Wang SJ, Zhang DL, Dang ZM (2017) Mechanical and dielectric properties of graphene incorporated polypropylene nanocomposites using polypropylene-graft-maleic anhydride as a compatibilizer. Compos Sci Technol 153:111–118. https://doi.org/10.1016/j.compscitech.2017.10.015
12. Infurna G, Teixeira PF, Dintcheva NT, Hilliou L, La Mantia FP, Covas JA (2020) Taking advantage of the functional synergism between carbon nanotubes and graphene nanoplatelets to obtain polypropylene-based nanocomposites with enhanced oxidative resistance. Eur Polym J 133:109796. https://doi.org/10.1016/j.eurpolymj.2020.109796
13. Tiwari SK, Sahoo S, Wang N, Huczko A (2020) Graphene research and their outputs: status and prospect. J Sci 5(1):10–29. https://doi.org/10.1016/j.jsamd.2020.01.006
14. Tariq S, Ali H, Akram M (2020) Thermal applications of hybrid phase change materials: a critical review. Therm Sci 24(3 Part B):2151–2169. https://doi.org/10.2298/tsci190302112t
15. Triantou M, Todorova N, Giannakopoulou T, Vaimakis T, Trapalis C (2017) Mechanical performance of re-extruded and aged graphene/polypropylene nanocomposites. Polym Int 66(12):1716–1724. https://doi.org/10.1002/pi.5353
16. Zhao X, Huang D, Ewulonu CM, Wu M, Wang C, Huang Y (2021) Polypropylene/graphene nanoplatelets nanocomposites with high conductivity via solid-state shear mixing. E Polym 21(1):520–532. https://doi.org/10.1515/epoly-2021-0039
17. Su Y, Li JJ, Weng GJ (2018) Theory of thermal conductivity of graphene-polymer nanocomposites with interfacial Kapitza resistance and graphene-graphene contact resistance. Carbon 137:222–233. https://doi.org/10.1016/j.carbon.2018.05.033
18. Xiao W, Zhai X, Ma P, Fan T, Li X (2018) Numerical study on the thermal behavior of graphene nanoplatelets/epoxy composites. Results Phys 9:673–679. https://doi.org/10.1016/j.rinp.2018.01.060
19. Wijerathne D et al (2023) Mechanical and thermal properties of graphene nanoplatelets-reinforced recycled polycarbonate composites. Int J Lightweight Mater Manuf 6(1):117–128. https://doi.org/10.1016/j.ijlmm.2022.09.001
20. Lee SJ, Yoon SJ, Jeon IY (2022) Graphene/Polymer nanocomposites: preparation, mechanical properties, and application. Polymers 14(21):4733. https://doi.org/10.3390/polym14214733
21. Fu S, Sun Z, Huang P, Li Y, Hu N (2019) Some basic aspects of polymer nanocomposites: a critical review. Nano Mater Sci 1(1):2–30. https://doi.org/10.1016/j.nanoms.2019.02.006
22. Bilisik K, Akter M (2021) Graphene nanocomposites: a review on processes, properties, and applications. J Ind Text 2021:152808372110242. https://doi.org/10.1177/15280837211024252
23. Yee K, Ghayesh MH (2023) A review on the mechanics of graphene nanoplatelets reinforced structures. Int J Eng Sci 186:103831. https://doi.org/10.1016/j.ijengsci.2023.103831
24. Liang JZ, Du Q (2018) Melt flow and flexural properties of polypropylene composites reinforced with graphene nano-platelets. Int Polym Process 33(1):35–41. https://doi.org/10.3139/217.3335
25. Sutar H, Mishra B, Senapati P, Murmu R, Sahu D (2021) Mechanical, thermal, and morphological properties of graphene nanoplatelet-reinforced polypropylene nanocomposites: effects of nanofiller thickness. J Compos Sci 5(1):24. https://doi.org/10.3390/jcs5010024
26. Armstrong G (2015) An introduction to polymer nanocomposites. Eur J Phys 36(6):063001. https://doi.org/10.1088/0143-0807/36/6/063001
27. Mukhopadhyay P, Gupta RK (2011) Trends and frontiers in graphene-based polymer nanocomposites. Plast Eng

67(1):32–42. https://doi.org/10.1002/j.1941-9635.2011.tb00669.x
28. Barangizi H, Pawlak A (2022) Crystallization of partially disentangled polypropylene in nanocomposites with aluminum oxide. Polymer 254:125049. https://doi.org/10.1016/j.polymer.2022.12504
29. Villasmil W, Fischer LJ, Worlitschek J (2019) A review and evaluation of thermal insulation materials and methods for thermal energy storage systems. Renew Sustain Energy Rev 103:71–84. https://doi.org/10.1016/j.rser.2018.12.040
30. Wang Y, Cheng L, Cui X, Guo W (2019) Crystallization behavior and properties of glass fiber reinforced polypropylene composites. Polymers 11(7):1198. https://doi.org/10.3390/polym11071198
31. Yang X, Chang J, Fang W, Yu Z, Li M, Li Q (2021) Improved impact property of long glass fiber-reinforced polypropylene random copolymer composites toughened with beta-nucleating agent via tunning the crystallization and phase. Polym Compos 42(7):3169–3183. https://doi.org/10.1002/pc.26047
32. Budai Z, Sulyok Z, Vargha V (2011) Glass-fibre reinforced composite materials based on unsaturated polyester resins. J Therm Anal Calorim 109(3):1533–1544. https://doi.org/10.1007/s10973-011-2069-5
33. Nikzad MK et al (2024) Thermo-mechanical properties of silica-reinforced PLA nanocomposites using molecular dynamics: the effect of nanofiller radius. J Polym Res 31(2):1–10. https://doi.org/10.1007/s10965-024-03873-0
34. Zhang M et al (2016) A review on polymer crystallization theories. Crystals 7(1):4. https://doi.org/10.3390/cryst7010004
35. Rafiee M, Nitzsche F, Laliberte J, Hind S, Robitaille F, Labrosse MR (2019) Thermal properties of doubly reinforced fiberglass/epoxy composites with graphene nanoplatelets, graphene oxide and reduced-graphene oxide. CompositesB 164:1–9. https://doi.org/10.1016/j.compositesb.2018.11.051
36. Wang Y, Hansen CJ, Wu CC, Robinette EJ (2021) Peterson AM (2021) Effect of surface wettability on the interfacial adhesion of a thermosetting elastomer on glass. RSC Adv 11(49):31142–31151. https://doi.org/10.1039/d1ra05916e
37. Urade AR, Lahiri I, Suresh KS (2022) Graphene properties, synthesis and applications: a review. JOM. https://doi.org/10.1007/s11837-022-05505-8
38. Pegoretti A, Mahmood H, Pedrazzoli D (2016) Kalaitzidou K (2016) Improving fiber/matrix interfacial strength through graphene and graphene-oxide nano platelets. IOP Conf Ser 139:012004. https://doi.org/10.1088/1757-899x/139/1/012004
39. Juan L (2020) Simultaneous improvement in the tensile and impact strength of polypropylene reinforced by graphene. J Nanomater 2020:1–5. https://doi.org/10.1155/2020/7840802
40. Nuruzzaman DM, Iqbal AK, Ismail NM, Ali MY, Iqbal AK, Hossain N (2023) Properties of glass fiber reinforced polyamide 6-polypropylene composites under tensile loading. In 8th Brunei International Conference on Engineering and Technology 2021. AIP Publishing. https://doi.org/10.1063/5.0110365.
41. Yallew TB, Kassegn E, Aregawi S, Gebresias A (2020) Study on effect of process parameters on tensile properties of compression molded natural fiber reinforced polymer composites. SN Applied Sciences, 2(3). https://doi.org/10.1007/s42452-020-2101-0.
42. Yao X et al (2021) Fabrication and mechanical performance of graphene nanoplatelet/glass fiber reinforced polymer hybrid composites. Front Mater 8:1–9. https://doi.org/10.3389/fmats.2021.773343
43. Ali I et al (2021) Effects of graphene nanoplatelets on mechanical and fire performance of flax polypropylene composites with intumescent flame retardant. Molecules 26(13):4094–4109. https://doi.org/10.3390/molecules26134094
44. Asoodeh F, Aghvami-Panah M, Salimian S, Naeimirad M, Khoshnevis H, Zadhoush A (2022) The effect of fibers' length distribution and concentration on rheological and mechanical properties of glass fiber–reinforced polypropylene Composite. J Ind Text 51(5):8452–8471. https://doi.org/10.1177/15280837211043254
45. Rafiee MA et al (2009) Enhanced mechanical properties of nanocomposites at low graphene content. ACS Nano 3(12):3884–3890. https://doi.org/10.1021/nn9010472
46. Chowdhury MA et al (2020) A review on tensile and flexural properties of fiber-reinforced polymer composites. J Polymer Textile Eng 7(5):16–26
47. Caixeta RV et al (2015) Influence of glass-fiber reinforcement on the flexural strength of different resin composites. Appl Adhesion Sci 3(1):1–6. https://doi.org/10.1186/s40563-015-0053-1
48. Ku H et al (2011) A review on the tensile properties of natural fiber reinforced polymer composites. Compos B Eng 42(4):856–873. https://doi.org/10.1016/j.compositesb.2011.01.010
49. Reddy MI et al (2018) Tensile and flexural properties of jute, pineapple leaf and glass fiber reinforced polymer matrix hybrid composites. Mater Today: Proc 5(1):458–462. https://doi.org/10.1016/j.matpr.2017.11.105
50. Barkoula NM et al (2009) Effect of compounding and injection molding on the mechanical properties of flax fiber polypropylene composites. J Reinf Plast Compos 29(9):1366–1385. https://doi.org/10.1177/0731684409104465
51. KC B et al (2017) Thermal and dimensional stability of injection-molded sisal-glass fiber hybrid PP biocomposites. J Polym Environ 26(3):1279–1289. https://doi.org/10.1007/s10924-017-1033-2

Publisher's Note Springer Nature remains neutral with regard to jurisdictional claims in published maps and institutional affiliations.

Springer Nature or its licensor (e.g. a society or other partner) holds exclusive rights to this article under a publishing agreement with the author(s) or other rightsholder(s); author self-archiving of the accepted manuscript version of this article is solely governed by the terms of such publishing agreement and applicable law.